Pregnane X receptor (PXR) activation: A mechanism for neuroprotection in a mouse model of Niemann–Pick C disease

S. Joshua Langmade*[†], Sarah E. Gale*[†], Andrey Frolov*, Ikuko Mohri[‡], Kinuko Suzuki[‡], Synthia H. Mellon[§], Steven U. Walkley[¶], Douglas F. Covey[∥], Jean E. Schaffer*, and Daniel S. Ory*[,**]

*Center for Cardiovascular Research, Department of Internal Medicine, and [∥]Department of Molecular Biology and Pharmacology, Washington University School of Medicine, St. Louis, MO 63110; [‡]Department of Pathology and Laboratory Medicine, University of North Carolina, Chapel Hill, NC 27599; [§]Department of Obstetrics, Gynecology, and Reproductive Sciences, University of California, San Francisco, CA 94143; and [¶]Department of Neuroscience, Albert Einstein College of Medicine, Bronx, NY 10461

Niemann–Pick type C1 (NPC1) disease is a fatal neurodegenerative disease characterized by neuronal lipid storage and progressive Purkinje cell loss in the cerebellum. We investigated whether therapeutic approaches to bypass the cholesterol trafficking defect in NPC1 disease might delay disease progression in the $npc1^{-/-}$ mouse model. We show that the neurosteroid allopregnanolone (ALLO) and T0901317, a synthetic oxysterol ligand, act in concert to delay onset of neurological symptoms and prolong the lifespan of $npc1^{-/-}$ mice. ALLO and T0901317 therapy preserved Purkinje cells, suppressed cerebellar expression of microglial-associated genes and inflammatory mediators, and reduced infiltration of activated microglia in the cerebellar tissue. To establish whether the mechanism of neuroprotection in $npc1^{-/-}$ mice involves GABA$_A$ receptor activation, we compared treatment of natural ALLO and ent-ALLO, a stereoisomer that has identical physical properties of natural ALLO but is not a GABA$_A$ receptor agonist. ent-ALLO provided identical functional and survival benefits as natural ALLO in $npc1^{-/-}$ mice, strongly supporting a GABA$_A$ receptor-independent mechanism for ALLO action. On the other hand, the efficacy of ALLO, ent-ALLO, and T0901317 therapy correlated with the ability of these compounds to activate pregnane X receptor-dependent pathways in vivo. These findings suggest that treatment with pregnane X receptor ligands may be useful clinically in delaying the progressive neurodegeneration in human NPC disease.

cholesterol | neurosteroid | allopregnanolone | neurodegeneration

Niemann–Pick type C (NPC) disease is an autosomal recessive neurodegenerative disorder characterized by accumulation of cholesterol and other lipids in the viscera and central nervous system and patterned Purkinje cell death in the cerebellum (1). Mutations in the NPC1 gene are responsible for ≈95% of human NPC disease. NPC1 loss-of-function mutants exhibit marked impairment of low-density lipoprotein (LDL) cholesterol esterification and mobilization of newly hydrolyzed LDL cholesterol to the plasma membrane (2–4), resulting in lysosomal sequestration of LDL cholesterol, delayed down-regulation of the LDL receptor and de novo cholesterol biosynthesis, and impaired ABCA1-mediated cholesterol efflux (5–7). Despite recent progress in characterizing the biochemical and genetic defects in NPC disease, the mechanisms underlying the neurodegenerative phenotype are not well understood. Moreover, at present there are no effective therapies that delay progression of human NPC disease.

Many of the prominent neuropathological features of human NPC disease [e.g., neuronal lipid storage and progressive loss of Purkinje neurons (1)] are recapitulated in the BALB/c NPC^{nih} ($npc1^{-/-}$) mouse, a naturally occurring murine model that harbors a retroposon insertion in the Npc1 gene (8, 9). In NPC1 mice, accumulation of unesterified cholesterol and gangliosides occurs in morphologically normal neurons as early as postnatal day 9 (P9) and precedes neuronal injury and cell loss (1, 10). Concomitant with

the lipid accumulation, brains of NPC1 mice exhibit microglial activation and infiltration and expression of proinflammatory mediators (10–12). Recent studies in chimeric NPC mice indicate that Purkinje cells undergo cell-autonomous neurodegeneration, suggesting that inflammation is not the initiating factor in Purkinje cell death, but rather a consequence of cell degeneration (12).

The lipid trafficking defects in NPC1 disease also affect cellular utilization of lipoprotein cholesterol (13, 14). In the $npc1^{-/-}$ mice, disruption of the NPC1-mediated cholesterol trafficking has a profound effect on neurosteroidogenesis, resulting in substantially less pregnenolone and allopregnanolone (ALLO) in the brains of $npc1^{-/-}$ mice as compared with WT mice (14). Administration of a single dose of the neurosteroid ALLO at P7 delays onset of neurological symptoms and prolongs survival in the $npc1^{-/-}$ mice (14). Curiously, the efficacy of ALLO treatment is progressively attenuated when administered at later points in postnatal development. Because the beneficial effect of ALLO on Purkinje cell survival is abrogated by treatment with a specific GABA$_A$ antagonist, it has been proposed that the survival benefit in the ALLO-treated mice may be mediated by GABA$_A$ receptor signaling.

NPC1 mutant cells also fail to appropriately use lipoprotein cholesterol for synthesis of 25-hydroxycholesterol and 27-hydroxycholesterol (13). These oxysterols reduce cellular cholesterol levels by suppressing sterol regulatory element-binding protein-dependent gene expression and by transcriptional activation of liver X receptor (LXR)-dependent pathways that promote cellular cholesterol efflux and catabolism (15, 16). Moreover, treatment of human NPC1 fibroblasts with 25-hydroxycholesterol or 27-hydroxycholesterol corrects sterol homeostatic defects and mobilizes cholesterol from the aberrant lysosomal compartment (13).

The defects in sterol homeostasis and in steroid and oxysterol synthesis led us to hypothesize that administration of a neurosteroid and a synthetic oxysterol ligand could mitigate NPC1 disease progression. Here we show that ALLO and the synthetic oxysterol ligand T0901317 act in concert to delay onset of neurological symptoms and prolong survival in the $npc1^{-/-}$ mouse model. We found that the Purkinje cell neuroprotection afforded by ALLO and T0901317 therapies correlates with the ability of these compounds to activate murine pregnane X receptor (PXR) in vivo. Our findings suggest that PXR ligands may be useful clinically in delaying neurodegeneration in human NPC disease.
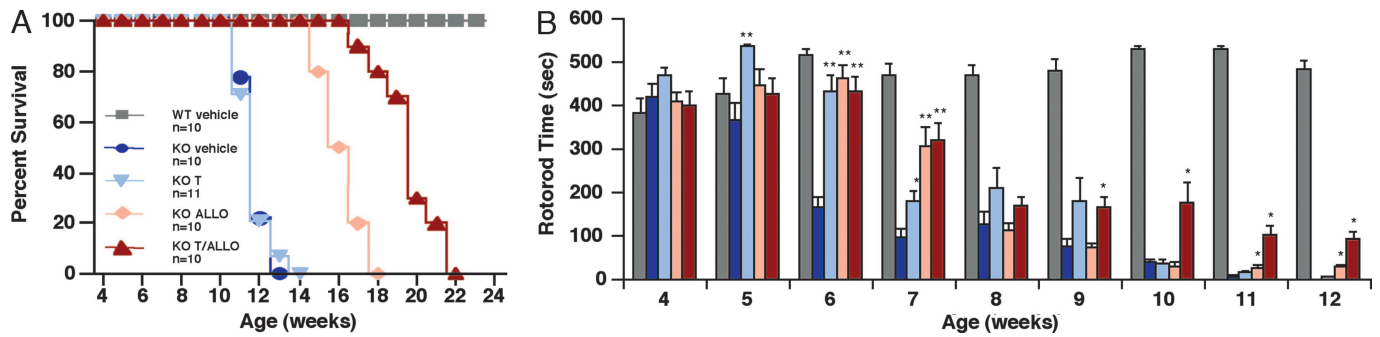

MEDICAL SCIENCES

Fig. 1. ALLO and T0901317 improve survival and neurological function in *npc1*^{−/−} mice. (*A*) Comparison of survival in WT and *npc1*^{−/−} mice: vehicle-treated, 78.8 days (*n* = 10); T0901317-treated, 79.9 days (*n* = 11, *P* = NS); ALLO-treated, 111.8 days (*n* = 10, *P* < 0.001); T0901317/ALLO-treated, 135.7 days (*n* = 10, *P* < 0.001). (*B*) Cerebellar function for each of the treatment groups was evaluated by measuring retention time on a rotating drum at 15 rpm. Cumulative retention time on the drum was determined for three consecutive attempts (maximum 180 s per attempt). Values represent mean for each group ± SEM. *, *P* ≤ 0.05; **, *P* ≤ 0.001 for compound-treated vs. vehicle-treated *npc1*^{−/−} mice.

Results

T0901317 and ALLO Therapy Improves Function and Survival in *npc1*^{−/−} Mice. In cell culture studies, we found that lipoprotein cholesterol-stimulated LXR gene activation is abrogated in NPC1-null cells (Fig. 7, which is published as supporting information on the PNAS web site). However, despite deficiency of endogenous oxysterol ligands (13), NPC1 mutants respond appropriately to exogenous LXR ligand activation. To extend these findings to an *in vivo* model of NPC1 disease, we investigated whether treatment of *npc1*^{−/−} mice with T0901317 can promote LXR target gene expression in brain tissue and thereby ameliorate disease progression. WT and *npc1*^{−/−} mice were randomized at P7 to injection with ALLO vs. vehicle alone and then treated at P18 with chow diet only or chow diet supplemented with T0901317. As shown previously by Griffin *et al.* (14), a single injection with ALLO at P7 improved survival in *npc1*^{−/−} mice by 42% (111.8 days in ALLO-treated mice vs. 78.8 days in vehicle-treated mice) (Fig. 1*A*). Although T0901317 therapy alone did not show increased survival, T0901317 treatment prolonged survival in ALLO-treated mice by 72% (135.7 days with combined treatment vs. 78.8 days in vehicle-treated mice). The survival benefit in the treated *npc1*^{−/−} mice was accompanied by improved neurological function. Treatment with either T0901317 or ALLO alone resulted in a functional improvement in the mice, delaying onset of neurological symptoms by 2 weeks and blunting decline in residual cerebellar function, whereas combined treatment with T0901317 and ALLO further slowed disease progression (Fig. 1*B*). Treatment with T0901317 and ALLO had no effect on survival or neurological function in WT mice (data not shown). Despite the significant functional and survival benefit in *npc1*^{−/−} mice, T0901317-treated mice showed evidence of toxicity, as demonstrated by failure to appropriately gain weight and by transient hepatic hypertriglyceridemia in P28 mice, which resolved in P49 mice and was likely due to the known induction of *de novo* lipogenesis by T0901317 (Fig. 8, which is published as supporting information on the PNAS web site).

T0901317 and ALLO Promote Purkinje Cell Survival. In light of the improved neurological function and survival benefit in the treated *npc1*^{−/−} mice, we examined the effect of ALLO and T0901317 therapy on preservation of cerebellar Purkinje cells. Purkinje cell number was reduced in vehicle-treated P63 mice by 83% as compared with WT mice (Fig. 2), with the greatest loss of Purkinje cells occurring in cerebellar lobes I–IV. Treatment with ALLO or T0901317 improved Purkinje cell survival by 53% and 75%, respectively, as compared with vehicle-treated mice. The greatest effect on Purkinje cell survival was in *npc1*^{−/−} mice treated with both ALLO and T0901317, in which the number of Purkinje neurons was increased 118% compared with untreated mice. In WT mice there was no difference in the number of Purkinje cell neurons in compound-treated vs. vehicle-treated mice (data not shown).

Effect of T0901317 and ALLO on Cerebellar Gene Expression. To gain insight into the mechanism by which T0901317 and ALLO therapy ameliorate progression of NPC disease, we examined cerebellar gene expression in the treated mice. Based on our cell culture studies (Fig. 7), we anticipated that treatment with T0901317 would increase expression of LXR target genes. We found that T0901317 therapy, alone or in combination with ALLO, led to induction of ABCA1 (7- to 9-fold), ABCG1 (2-fold), and sterol regulatory element-binding protein 1c (5- to 6-fold) gene expression in P28
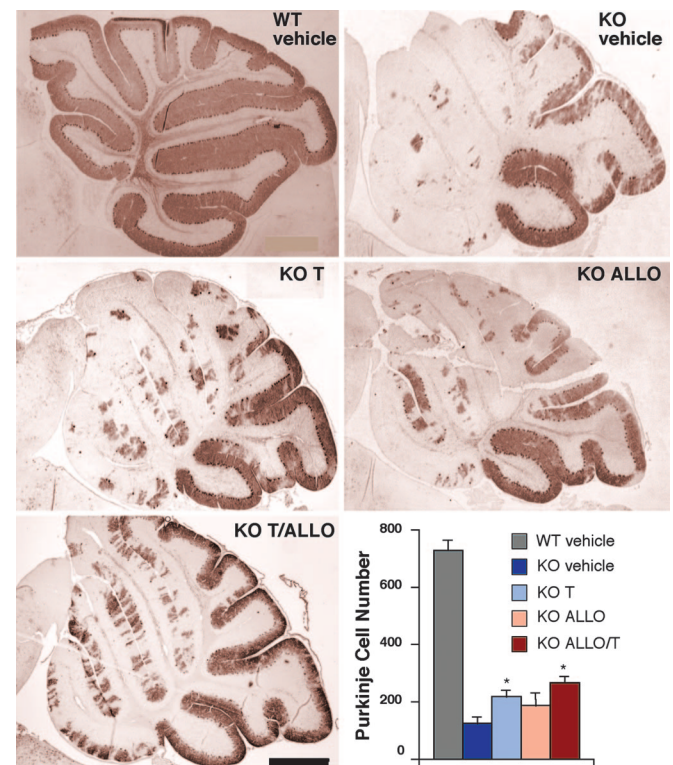

Fig. 2. Purkinje cell survival is increased in ALLO- and T0901317-treated *npc1*^{−/−} mice. Shown are calbindin-immunoreactive Purkinje cells in midline cerebellum sections from 63-day-old *npc1*^{−/−} mice. (Scale bar: 500 μm.) *Bottom Right* shows quantification of calbindin-immunoreactive Purkinje cell bodies in cerebellar sections (*n* = 3–5 mice per treatment group). Results are means ± SEM. *, *P* ≤ 0.05 for compound-treated vs. vehicle-treated *npc1*^{−/−} mice.
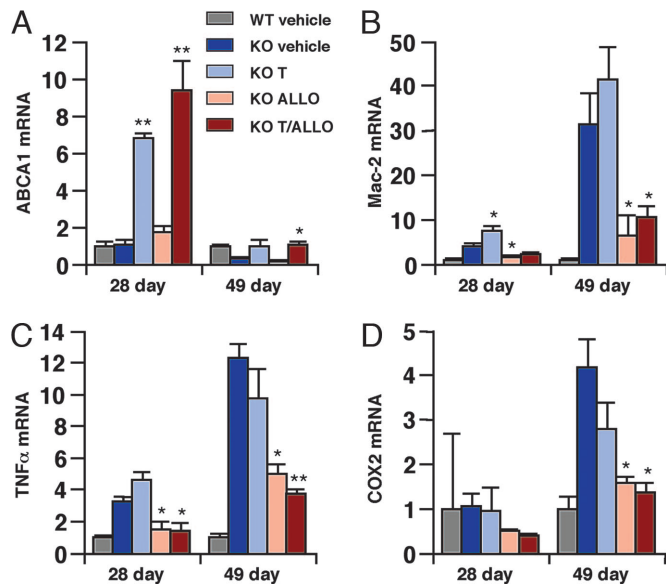
Fig. 3. Cerebellar expression of LXR regulated genes and microglial and inflammatory markers in response to treatment. Expression of ABCA1, Mac-2, TNFα, and cyclooxygenase 2 in the cerebella of 28-day-old and 49-day-old mice was determined by real-time quantitative RT-PCR. Expression is shown as fold induction relative to vehicle-treated WT mice. Values represent the mean ± SEM of three mice per group (triplicate determinations for each mouse). *, $P \le$ 0.05; **, $P \le$ 0.01 for compound-treated vs. vehicle-treated $npc1^{-/-}$ mice.

Fig. 4. T0901317 and ALLO promote Purkinje cell survival in $npc1^{-/-}$ mice. Cerebellar sections from 49-day-old WT mice (*Top*), vehicle-treated $npc1^{-/-}$ mice (*Middle*), and T0901317 and ALLO-treated $npc1^{-/-}$ mice (*Bottom*) were stained with antibodies to CD68 (green) and calbindin (red) and with a nuclear stain, Hoechst dye 33342 (blue in *Left*), and examined by immunofluorescence. The asterisk and diamond denote granule and Purkinje cell layers, respectively. Arrowheads indicate calbindin-stained Purkinje cell bodies. Omission of the nuclear stain (*Right*) facilitates visualization of microglia within the granule cell layer. (Scale bar: 200 μm.)

mouse cerebella (Fig. 3 and Fig. 9 *A* and *B*, which is published as supporting information on the PNAS web site). Monotherapy with ALLO, which fails to activate LXR in cell-based reporter assays (data not shown), did not induce expression of the LXR target genes in the cerebellum. The effect of T0901317 treatment on P49 mice was less pronounced, possibly because of the progressive neuronal loss (Figs. 3 and 9*B*). These observations suggest that dietary T0901317 (50 mg/kg per day) achieves sufficient drug levels in cerebellar tissue of the $npc1^{-/-}$ mice to activate LXR target genes and is in agreement with earlier *in vivo* studies with T0901317 (17).

Because the progressive neurodegeneration in NPC disease is accompanied by microglial infiltration in the cerebellum (11, 12), we monitored for the presence of microglia by examining expression of microglial-associated genes in the $npc1^{-/-}$ mice. In vehicle-treated mice, there was dramatic expression of multiple microglial markers, which correlated with disease progression, i.e., greater in the P49 mice than in the P28 mice (Figs. 3 and 9 *C–E*). Expression of these markers was suppressed in T0901317-treated (Mac-1a) and ALLO-treated (Mac-2 and Mac-1a) P49 mice, and the effects were additive in the combined therapy group. We also monitored for production of proinflammatory mediators in cerebellar tissue of the $npc1^{-/-}$ mice by measuring gene expression. In vehicle-treated mice, expression of the microglial-associated genes was accompanied by increased expression of proinflammatory cytokines (TNFα and IL1-β), cytokine receptors (TNFRp55), and inflammatory mediators (cyclooxygenase 2) (Figs. 3 *C* and *D* and 9 *F* and *G*). Expression of these inflammatory mediator genes was less apparent in the P28 mice than in the P49 mice, consistent with the expression pattern for the microglial markers. Treatment with ALLO, but not T0901317, decreased expression of these genes, whereas combined therapy was most effective for suppression of the inflammatory mediators.

T0901317 and ALLO Attenuate Microglial Infiltration and Purkinje Cell Loss. We next examined whether the attenuated expression of the microglial-associated genes and inflammatory mediators in the treatment groups reflected reduced infiltration of activated micro-
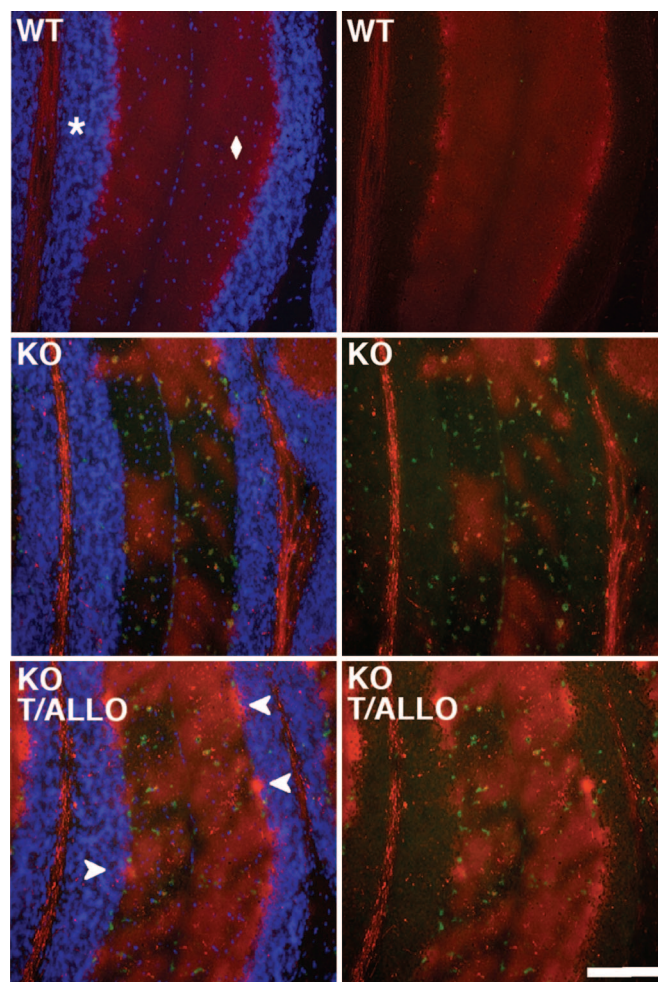
glia in the cerebellar tissue. Cerebellar sections from P49 $npc1^{-/-}$ mice were stained for calbindin, a specific marker of Purkinje cell neurons, and CD68, a microglial marker. In vehicle-treated mice there was an ≈50% loss of Purkinje cell bodies in cerebellar lobes III and IV, as compared with WT mice (Fig. 4). Strikingly, loss of Purkinje neurons occurred precisely in regions of the Purkinje cell layer that were infiltrated with CD68-positive microglial cells. In the vehicle-treated $npc1^{-/-}$ mice, Purkinje cell loss and microglial cell infiltration were least apparent in lobes IX and X, the region of the cerebellum that is generally preserved even in late-stage NPC disease (8) (Fig. 2 and Fig. 10, which is published as supporting information on the PNAS web site). T0901317 and ALLO treatment improved Purkinje cell survival and attenuated microglial cell infiltration in both the granule and Purkinje cell layers (Fig. 4). T0901317 or ALLO treatment alone similarly prevented Purkinje cell loss, although the effect in these groups was less pronounced than in the combined therapy group (data not shown).

Enantiomer of ALLO Prolongs Survival in $npc1^{-/-}$ Mice. ALLO has been proposed to exert its anesthetic effect through binding to
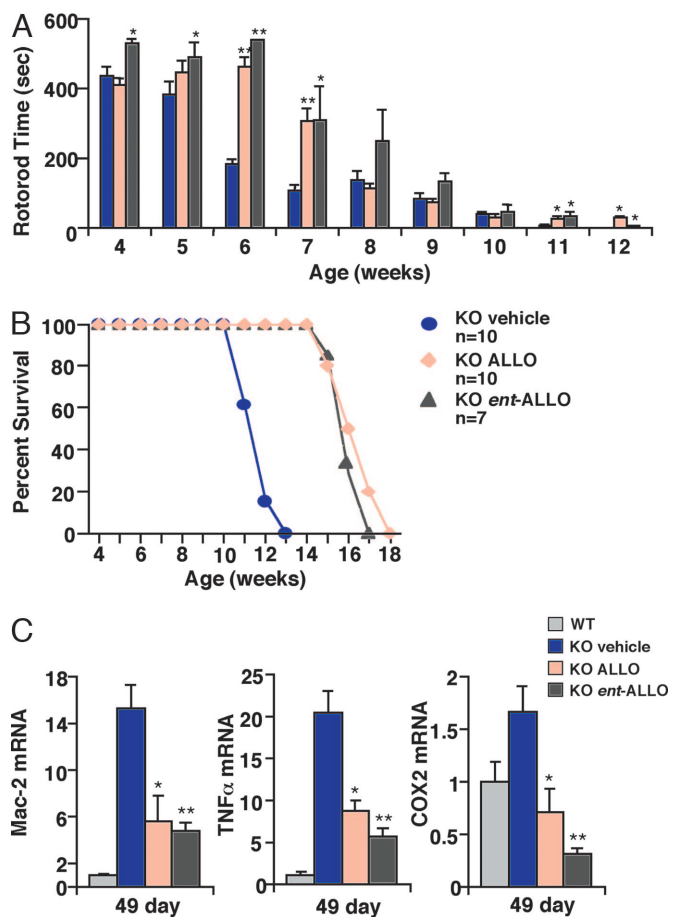
Fig. 5. *ent*-ALLO provides neuroprotection and prolongs survival in *npc1*$^{-/-}$ mice. *ent*-ALLO injected into P7 mice resulted in motor skill improvements (*A*) and survival (*B*) similar to those seen in mice injected with the natural form of ALLO. *ent*-ALLO-injected animals showed similar reductions in Mac-2, TNFα, and cyclooxygenase 2 gene expression as compared with levels in ALLO-injected mice (*C*). Expression is shown as fold induction relative to vehicle-treated WT mice. Values represent the mean ± SEM. *, $P \leq 0.05$; **, $P \leq 0.001$ for compound-treated vs. vehicle-treated *npc1*$^{-/-}$ mice.

specific steroid recognition sites on the GABA$_A$ receptor (18). To investigate whether activation of GABA$_A$ receptors is required for ALLO-mediated neuroprotection in *npc1*$^{-/-}$ mice, we synthesized the enantiomer of ALLO (*ent*-ALLO) (19), a stereoisomer of ALLO in which the absolute configuration of all eight chiral centers is inverted (Fig. 11*A*, which is published as supporting information on the PNAS web site). *ent*-ALLO has physical properties and interacts with membranes in a manner identical to that of natural ALLO but has a much lower affinity (>100-fold) for GABA$_A$ receptors and fails to modulate receptor function (18). Accordingly, P7 mice treated with natural ALLO uniformly slept for 40–45 min after injection because of its anesthetic properties, whereas mice injected with the same dose of *ent*-ALLO did not show evidence of anesthetic effect. Administration of *ent*-ALLO at P7 delayed onset of neurological symptoms and preserved cerebellar function in *npc1*$^{-/-}$ mice to the same extent as treatment with natural ALLO (Fig. 5*A*). *ent*-ALLO therapy also resulted in similar body weight profiles and conferred identical survival benefits (mean survival 111.8 ± 2.0 days for natural ALLO vs. 109.9 ± 1.8 days for *ent*-ALLO), as compared with the natural ALLO-treated mice (Fig. 5*B* and Fig. 12, which is published as supporting information on the PNAS web site). Moreover, like the natural neurosteroid, *ent*-ALLO treatment suppressed expression of microglial-associated genes and proinflammatory mediators (Fig. 5*C*). Thus,

ALLO likely modulates disease progression in the mouse model through a GABA$_A$ receptor-independent mechanism.

ALLO Activates PXR-Dependent Gene Expression in *npc1*$^{-/-}$ Mice. Because both natural ALLO and *ent*-ALLO provided similar neuroprotection and survival benefit in *npc1*$^{-/-}$ mice, we reasoned that the enantiomeric pair must exert their effects through a common mechanism. In light of the previous identification of ALLO as a PXR activator and the role of PXR in the induction of CYP3A isoforms in Purkinje neurons in cerebellar tissue (20, 21), we tested the hypothesis that ALLO might promote neuronal survival through activation of PXR target genes. Using a CYP3A4 promoter reporter construct (22), we found that both natural ALLO and *ent*-ALLO activated human PXR (hPXR)- and murine PXR (mPXR)-dependent gene expression (Fig. 6*A* and Fig. 13*A*, which is published as supporting information on the PNAS web site). The EC$_{50}$ for activation of mPXR by natural ALLO and *ent*-ALLO was 1 and 2 μM, respectively, ≈5-fold lower than for activation of hPXR by natural ALLO. Consistent with a prior report, T0901317 also activated mPXR with an EC$_{50}$ of 0.075 μM (Fig. 7*B*), which is well below the tissue concentration achieved at 50 mg/kg per day of dosing (17). Activation by ALLO enantiomers was specific for PXR, because these compounds were unable to activate other nuclear receptors in *in vitro* reporter assays (M. Ricketts, D. Moore, and D.S.O., unpublished results). To determine whether administration of ALLO induces cerebellar expression of PXR target genes *in vivo*, we treated *npc1*$^{-/-}$ mice at P7 with either natural ALLO or *ent*-ALLO, harvested cerebellar tissue from 8 to 72 h after injection, and measured expression of PXR target genes. We found that the enantiomeric pair induced expression of the CYP3A13, a cerebellar P450 isoform that may be involved in sterol catabolism and detoxification (20, 21). CYP3A13 expression peaked at 24 h in the treated mice and returned to baseline at 72 h after injection (Fig. 6*B*). Expression levels at 24 h were comparable between WT and vehicle-treated *npc1*$^{-/-}$ mice (data not shown). Unexpectedly, we found that CYP3A13 expression was significantly increased in cerebellar tissue of P28 *npc1*$^{-/-}$ mice that had received a single injection of ALLO at P7 (Fig. 6*C*). We similarly observed induction of CYP3A13 expression in T0901317-treated mice, demonstrating that T0901317 activates mPXR *in vivo*.

Discussion

In NPC1 disease models, oxysterol and steroid synthesis is impaired, suggesting that failure to deliver lipoprotein cholesterol to sites of utilization may disrupt multiple cellular processes and contribute to disease pathogenesis (13, 14). In the present study we investigated whether therapeutic approaches to bypass the cholesterol trafficking defect caused by NPC1 loss of function might ameliorate disease progression in the *npc1*$^{-/-}$ mouse model. We show that the neurosteroid ALLO and T0901317 act in concert to delay onset of neurological symptoms and significantly prolong survival of *npc1*$^{-/-}$ mice. ALLO and T0901317 therapy attenuated Purkinje cell loss, suppressed expression of microglial-associated genes and inflammatory mediators in the cerebellum, and reduced infiltration of activated microglia in the cerebellar tissue. The functional and survival benefit conferred by ALLO and T0901317 treatment correlated with the ability of these compounds to activate PXR-dependent pathways *in vivo*. We propose that PXR ligands may be useful clinically to delay neurodegeneration in human NPC disease.

The pathogenesis of neurodegeneration in NPC1 disease is not well understood. In the *npc1*$^{-/-}$ mouse model, significant neuronal cholesterol accumulation precedes the appearance of activated glial cells and neuronal cell loss (10). The stimulus for glial cell recruitment has not been established, but it may result from neuronal injury caused by accumulation of toxic lipid species or reduced levels of cholesterol-derived metabolites in *npc1*$^{-/-}$ Purkinje cells. A recent study employing chimeric *npc1*$^{-/-}$ mice demonstrated that
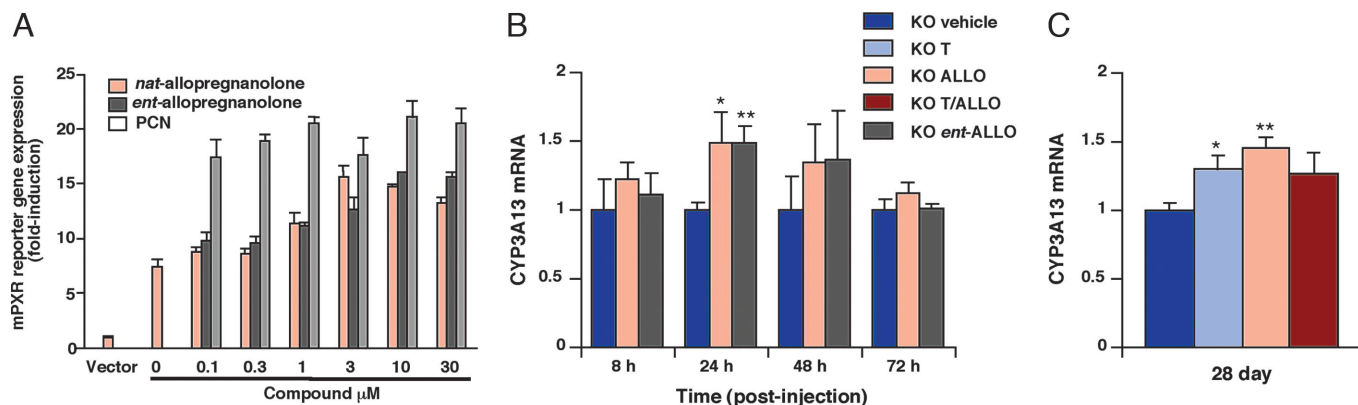
Fig. 6. ALLO activates PXR target genes *in vitro* and *in vivo*. (*A*) Cells were transfected with XREM-CYP3A4-LUC reporter construct, pTK-*Renilla*, pSG5-mPXR, and hHNF4α. Vector indicates transfection with XREM-CYP3A4-LUC and pTK-*Renilla* alone. Cells were treated for 24 h with ALLO and *ent*-ALLO. Pregnenolone-16α-carbonitrile (PCN) serves as a control for activation of mPXR. (*B*) ALLO and *ent*-ALLO activate the PXR target gene CYP3A13 in cerebellar tissue of P7 *npc1*$^{-/-}$ mice. (*C*) Expression of CYP3A13 is induced at 28 days in *npc1*$^{-/-}$ mice injected with ALLO at P7 and in T0901317-treated mice. Expression is shown as fold induction relative to vehicle-treated *npc1*$^{-/-}$ mice. Values represent the mean ± SEM of four mice per group (triplicate determinations for each mouse). *, $P \leq 0.05$; **, $P \leq 0.01$ for compound-treated vs. vehicle-treated mice.

in cerebellar tissue neighboring WT Purkinje cells were unaffected by the robust inflammatory response, suggesting that the microglial-mediated inflammation specifically targeted *npc1*$^{-/-}$ Purkinje cells in the cerebella of chimeric mice (12). In our study we found extensive infiltration of activated microglia in both the Purkinje cell and granule cell layers in *npc1*$^{-/-}$ mice, which is in agreement with previous reports (10–12). We further show that the recruitment of microglia and expression of proinflammatory mediators were suppressed by ALLO and T0901317 treatment and resulted in improved Purkinje cell survival. It is possible that these compounds, through modulating trafficking and utilization of lipoprotein cholesterol, protect *npc1*$^{-/-}$ Purkinje cells by attenuating the autonomous signal that identifies *npc1*$^{-/-}$ neurons as "damaged" or by masking recognition of *npc1*$^{-/-}$ neurons by microglia. Alternatively, ALLO and T0901317 may preserve *npc1*$^{-/-}$ Purkinje cells by directly modulating glial cell behavior with respect to activation and recruitment to damaged neurons.

Previous studies have shown that ALLO therapy promotes Purkinje cell survival and increases lifespan in *npc1*$^{-/-}$ mice (14, 23). Griffin *et al.* (14) proposed that ALLO may exert its effects through GABA$_A$ receptor signaling because ALLO is a GABA$_A$ receptor agonist and the beneficial effects of ALLO on survival of cultured Purkinje cells were blocked by bicuculline, a GABA$_A$ receptor antagonist. To establish whether the mechanism of ALLO-mediated neuroprotection involves GABA$_A$ receptor activation, we compared treatment of natural ALLO and *ent*-ALLO in *npc1*$^{-/-}$ mice. *ent*-ALLO, which is not a GABA$_A$ receptor agonist (18), provided functional and survival benefits identical to those of the natural compound in the *npc1*$^{-/-}$ mice, strongly supporting a GABA$_A$ receptor-independent mechanism for ALLO. Given that natural ALLO and *ent*-ALLO interact with membranes in an identical manner (18), it is possible that the neuroprotective effects of these compounds are mediated through direct steroid–membrane interactions. On the other hand, ALLO, which has been shown to activate PXR *in vitro* (21), may exert its effects in *npc1*$^{-/-}$ mice through activation of PXR target genes. Our finding that natural ALLO and *ent*-ALLO lead to rapid induction of the CYP3A13 P450 isoform in cerebellar tissue of P7 *npc1*$^{-/-}$ mice suggests that PXR activation may be involved in Purkinje cell neuroprotection. The lack of enantioselectivity of PXR for the ALLO stereoisomers is not altogether surprising. In contrast to many other nuclear receptors, PXR exhibits broad ligand specificity for xenobiotics and endogenous compounds and possesses a large, flexible binding cavity capable of docking single ligands in multiple orientations (24). Overlay of the three-dimensional structures of the

ALLO enantiomeric pair reveals that, when the steroid rings are kept coplanar, the polar groups at the 3 and 20 positions can be superimposed. Thus, *ent*-ALLO may be able to adopt an orientation similar to the natural compound that permits coordination of the polar residues lining the PXR binding cavity, which are critical for pharmacologic activation (Fig. 11*B*).

Activation of PXR target genes may also explain the improvement in functional status and preservation of Purkinje cells in the *npc1*$^{-/-}$ mice treated with T0901317. Although the benefits of the nonselective LXR ligand may relate to induction of LXR target gene expression involved in cholesterol efflux and catabolism or to suppression of inflammatory mediators, T0901317 is also capable of activating PXR-dependent gene expression (25). In fact, we found that T0901317 activated mPXR *in vitro* at an EC$_{50}$ 13-fold less than ALLO and, like ALLO, induced PXR target gene expression in cerebellar tissue in P28 *npc1*$^{-/-}$ mice. When T0901317 was administered to ALLO-treated mice, their lifespan was further extended by 21%. Dietary administration of T0901317, therefore, may afford neuroprotection in the *npc1*$^{-/-}$ mice through dual activation of LXR and PXR targets or possibly by providing for sustained PXR activation, similar to the benefits of weekly injections with ALLO (23) (S.H.M., unpublished results).

A puzzling aspect of the neuroprotective effects of ALLO is how a single injection of the neurosteroid in *npc1*$^{-/-}$ mice can prolong survival by ≈40% in P7 mice but provide no appreciable benefit in P23 mice (14). We demonstrate that PXR-regulated gene expression in cerebellar tissue of ALLO-treated P7 mice is bimodal. CYP3A13 expression initially peaks at 24 h and returns to basal levels at 72 h but is reexpressed in P28 mice. A possible explanation for this pattern of gene expression is perinatal imprinting, in which early exposure to a drug results in latent gene expression. Such a mechanism is supported by a recent report in which neonatal rats exposed to phenobarbital within the first 7 days of life exhibit increased postpubertal expression of both constitutive and inducible P450 isoforms (26). The plasticity in neonates (e.g., P7 mice), in contrast to adults, may render them susceptible to genetic programming that alters levels of P450-dependent metabolizing enzymes. How would increased expression of P450 isoforms confer a survival benefit in *npc1*$^{-/-}$ mice? Whereas synthesis of side-chain oxygenated cholesterol is decreased in NPC1 mutants, there is a dramatic increase in *npc1*$^{-/-}$ mouse tissues in the levels of nonenzymatic cholesterol oxidation products (27), which have been reported to be potentially cytotoxic and proapoptotic. Thus, induction of PXR-regulated P450 isoforms may serve a critical role in

MEDICAL SCIENCES

detoxification of cholesterol oxidation products, thereby mitigating neuronal injury.

In the present study we provide insight into the mechanism through which ALLO delays onset of neurological symptoms and prolongs survival in $npc1^{-/-}$ mice. Our finding that ALLO induces expression of PXR targets *in vivo* suggests a role for PXR activation in protection of Purkinje cells. Future treatment trials will need to be performed in $npc1^{-/-}$ $pxr^{-/-}$ double knockout mice to definitively establish whether PXR activation is required for ALLO-mediated neuroprotection. The possibility that PXR activation is neuroprotective in $npc1^{-/-}$ mice has important implications for development of therapeutic approaches to delay progression of NPC1 disease. hPXR is activated by number of commonly used drugs, including rifampicin, phenytoin, and hyperphorin, a constituent of St. John's wort (24), and the ready availability of such clinically approved compounds could facilitate therapeutic trials in human NPC subjects.

Methods

Mice. BALB/c NPC^{nih} mice were obtained from the Jackson Laboratory (Bar Harbor, ME). P7 mice received a single s.c. injection of 25 mg/kg ALLO (5α-pregnan-3α-ol-20-one; Research Plus, Manasquan, NJ) or 25 mg/kg *ent*-ALLO (19) in 20% 2-hydroxypropyl-β-cyclodextrin as described (14). Mice were weaned at P18 and fed either a standard chow diet or a standard chow diet containing 50 mg/kg T0901317 compound per day (Cayman Chemical, Ann Arbor, MI).

Protein Preparation and Western Blot Analysis. Microsomal proteins from normal (CRL-1474; American Type Culture Collection, Manassas, VA) and NPC1-null fibroblasts (NPC1^{1628delC}, NIH 98.016) were prepared as previously described (3). Protein samples were resolved by SDS/PAGE, and Western blot analysis was performed as previously described (3). For ABCA1 detection, a rabbit polyclonal antibody to human ABCA1 (1:500; Novus Biologicals, Littleton, CO) and an anti-rabbit-HRP secondary antibody were used.

Cholesterol Efflux Assay. Fibroblasts were labeled by 1 μCi/ml (1 Ci = 37 GBq) [1,2-^{3}H(N)]-cholesterol (PerkinElmer, Boston, MA) incubated in the presence and absence of 10 μM T0901317 and 10 μM 9-*cis*-retinoic acid, and efflux was performed as described (28). Cholesterol efflux was expressed as the percentage of the radioactivity released from the cells into the medium divided by total radioactivity in cells and media.

Immunocytochemistry. Tissue sections from paraformaldehyde-fixed brains were processed and stained with anti-calbindin D-28K as described (29). Quantification of Purkinje cells was performed by counting the total number of calbindin-immunoreactive cell bodies in the Purkinje cell layer.

Real-Time Quantitative RT-PCR. RNA isolation, cDNA synthesis, and real-time quantitative RT-PCR using SYBR Green Master Mix or TaqMan Fast Universal PCR Master Mix with template-specific primers (Table 1, which is published as supporting information on the PNAS web site) were performed as described (30). Fold changes in gene expression for a particular target were determined as previously described and normalized to 36B4 expression.

Immunofluorescence Microscopy. Fixed cerebellum sections were incubated overnight with rat polyclonal anti-mouse CD68:FITC (1:1,000; Serotec, Raleigh, NC) and rabbit polyclonal anti-calbindin D-28K (1:1,000; Chemicon International, Temecula, CA). The calbindin antibody was detected through incubation for 1 h with goat anti-rabbit Alexa Fluor 647 (1:1,000; Molecular Probes, Carlsbad, CA). Sections were then incubated with Hoechst dye 33342 (Molecular Probes) at a concentration of 10 μg/ml before drying the slides and mounting. Fluorescent images were captured by using an Axioskop 2 microscope (Zeiss) and analyzed with Axiovision 4 software.

Transient Transfection Assays. Transfection assays with Chinese hamster ovary cells were performed as described (21) with 25 ng of XREM-CYP3A4-LUC (22), 13 ng of pTK-*Renilla* as a transfection control (13), 13 ng of pSG5-hPXR (31), 13 ng of pSG5-mPXR (gift of Bryan Goodwin, GlaxoSmithKline, Research Triangle Park, NC), and 13 ng of hHNF4α (21). Cells were incubated in the presence and absence of ALLO, *ent*-ALLO, T0901317, or pregnenolone-16α-carbonitrile. Cells were lysed, and luciferase activity was determined. Values represent the average of quadruplicate determinations of independently transfected wells.

Statistics. All results are expressed as mean ± SEM. The statistical significance of differences in mean values was determined by single-factor ANOVA.

1. Walkley SU, Suzuki K (2004) *Biochim Biophys Acta* 1685:48–62.
2. Neufeld EB, Cooney AM, Pitha J, Dawidowicz EA, Dwyer NK, Pentchev PG, Blanchette-Mackie EJ (1996) *J Biol Chem* 271:21604–21613.
3. Millard EE, Srivastava K, Traub L, Schaffer JE, Ory DS (2000) *J Biol Chem* 275:38445–38451.
4. Wojtanik KM, Liscum L (2003) *J Biol Chem* 278:14850–14856.
5. Liscum L, Faust JR (1987) *J Biol Chem* 262:17002–17008.
6. Pentchev PG, Comly ME, Kruth HS, Vanier MT, Wenger DA, Patel S, Brady RO (1985) *Proc Natl Acad Sci USA* 82:8247–8251.
7. Choi HY, Karten B, Chan T, Vance JE, Greer WL, Heidenreich RA, Garver WS, Francis GA (2003) *J Biol Chem* 278:32569–32577.
8. Higashi Y, Murayama S, Pentchev PG, Suzuki K (1993) *Acta Neuropathol* 85:175–184.
9. Loftus SK, Morris JA, Carstea ED, Gu JZ, Cummings C, Brown A, Ellison J, Ohno K, Rosenfeld MA, Tagle DA, *et al.* (1997) *Science* 277:232–235.
10. Reid P, Sakahita N, Sugii S, Ohno-Iwashita Y, Shimada Y, Hickey W, Chang T (2004) *J Lipid Res* 45:582–591.
11. Wu Y-P, Mizukami H, Matsuda J, Saito Y, Proia R, Suzuki K (2005) *Mol Genet Metab* 84:9–17.
12. Ko D, Milenkovic L, Beier S, Manuel H, Buchanan J, Scott M (2005) *PLoS Genet* 1:81–95.
13. Frolov A, Zielinski SE, Crowley JR, Dudley-Rucker N, Schaffer JE, Ory DS (2003) *J Biol Chem* 278:25517–25525.
14. Griffin L, Gong W, Verot L, Mellon S (2004) *Nat Med* 10:704–711.
15. Janowski BA, Willy PJ, Devi TR, Falck JR, Manglesdorf DJ (1996) *Nature* 383:728–731.
16. Fu X, Menke JG, Chen Y, Zhou G, MacNaul KL, Wright SD, Sparrow CP, Lund EG (2001) *J Biol Chem* 276:38378–38387.
17. Whitney KD, Watson MA, Collins JL, Benson WG, Stone TM, Numerick MJ, Tippin TK, Wilson JG, Winegar DA, Kliewer SA (2002) *Mol Endocrinol* 16:1378–1385.
18. Wittmer L, Hu Y, Kalbrenner M, Evers A, Zorumski C, Covey D (1996) *Mol Pharmacol* 50:1581–1586.
19. Hu Y, Wittmer L, Kalkbrenner M, Evers A, Zorumski C, Covey D (1997) *J Chem Soc Perkin Trans 1* 3665–3671.
20. Hagemeyer C, Rosenbrock H, Ditter M, Knoth R, Volk B (2003) *Neuroscience* 117:521–529.
21. Lamba V, Yasuda K, Lamba J, Assem M, Davila J, Strom S, Schuetz E (2004) *Toxicol Appl Pharmacol* 199:251–265.
22. Goodwin B, Hodgson E, Liddle C (1999) *Mol Pharmacol* 56:1329–1339.
23. Ahmad I, Lope-Piedrafta S, Bi X, Hicks C, Yao Y, Yu C, Chaitkin E, Howison C, Weberg L, Trouard T, Erickson R (2005) *J Neurosci Res* 82:811–821.
24. Watkins R, Wisely G, Moore L, Collins J, Lambert M, Williams S, Willson T, Kliewer SA, Redinbo M (2001) *Science* 292:2329–2333.
25. Shenoy S, Spencer T, Mercer-Haines N, Alipour M, Gargano M, Runge-Morris M, Kocarek T (2004) *Drug Metab Dispos* 32:66–71.
26. Agrawal A, Shapiro B (2005) *FASEB J* 19:470–472.
27. Tint G, Pentchev P, Xu G, Batta A, Shiefer S, Salen G, Honda A (1998) *J Inherited Metab Dis* 21:853–863.
28. Chen W, Sun Y, Welch C, Gorelik A, Leventhal AR, Tabas I, Tall AR (2001) *J Biol Chem* 276:43564–43569.
29. Matsuda J, Kido M, Tadano-Aritomi K, Ishizuka I, Takeda E, Suzuki K, Kuroda Y (2004) *Hum Mol Genet* 13:2709–2723.
30. Millard E, Gale S, Dudley N, Zhang J, Schaffer J, Ory D (2005) *J Biol Chem* 280:28581–28590.
31. Lehmann J, McKee D, Watson M, Willson T, Moore J, Kliewer S (1998) *J Clin Invest* 102:1016–1023.